Frontiers in Bioscience Landmark

Front. Biosci. (Landmark Ed) **2024**; 29(3): 115
https://doi.org/10.31083/j.fbl2903115

Original Research

Interferon Regulatory Factor 4 (IRF4) Plays a Key Role in Osteoblast Differentiation of Postmenopausal Osteoporosis

Xuan Wu[1,†], Cuicui Yang[2,†], Xiangxu Chen[1], Zhengming Shan[1], Xiaotao Wu[1,*]

[1]Department of Orthopedics, Zhong Da Hospital, School of Medicine, Southeast University, 210009 Nanjing, Jiangsu, China
[2]Research Center for Bone and Stem Cells; Key Laboratory for Aging & Disease; Nanjing Medical University, 211166 Nanjing, Jiangsu, China
*Correspondence: wuxiaotaospine@seu.edu.cn (Xiaotao Wu)
[†]These authors contributed equally.

Academic Editor: Elisa Belluzzi
Submitted: 22 September 2023 Revised: 14 December 2023 Accepted: 27 December 2023 Published: 20 March 2024

Abstract

Background: Postmenopausal osteoporosis (PMOP) is a prevalent disease, which features decreased bone mass, bone weakness and deteriorated bone microstructure in postmenopausal women. Although many factors have been revealed to contribute to the occurrence of PMOP, its mechanism remains undefined. This work aimed to identify significant changes in gene expression during PMOP formation and to examine the most valuable differential genes in postmenopausal osteoporosis versus the control group. **Methods**: The GSE68303 dataset that contains 12 ovariectomize (OVX) experimental and 11 sham groups was downloaded and analyzed. The results indicated that interferon regulatory factor 4 (*IRF4*) might be a hub gene in the development of postmenopausal osteoporosis. Western blot and immunohistochemistry were carried out to evaluate IRF4 levels in thoracic vertebra extracts from OVX and Sham mice. To assess IRF4's impact on osteogenic differentiation in postmenopausal bone marrow mesenchymal stem cells (BM-MSCs), IRF4 overexpression (OV-IRF4) and knockdown (Sh-IRF4) plasmids were constructed. **Results**: The results showed that comparing with the sham group, bone samples from the OVX group showed higher IRF4 expression. Alkaline phosphatase (ALP) staining revealed that IRF4 overexpression significantly inhibited ALP activity, while IRF4 knockdown promoted ALP activity in BM-MSCs. Simvastatin-treated OVX mice showed increased total bone volume/total tissue volume (BV/TV) and elevated Runx2 expression by immunohistochemical staining compared with the OVX group. **Conclusions**: This study demonstrated that IRF4 is associated with OVX induced osteoporosis, it can regulate bone stability by inhibiting the osteogenic differentiation BM-MSCs. This study may help enhance our understanding of the molecular mechanism of PMOP formation, providing new insights into estrogen defiance induced osteoporosis.

Keywords: osteoporosis; OVX; IRF4; simvastatin

1. Introduction

Postmenopausal osteoporosis (PMOP) is a type of primary osteoporosis [1]. With the increasingly aging society, osteoporosis is considered a health threat seriously affecting middle-aged and elderly women globally and imposing a heavy burden on governments and medical systems [2]. PMOP is mainly caused by the lack of estrogen after menopause. Monitoring the genetic changes associated with bone resorption and bone formation disorders by assessing gene expression alterations in postmenopausal osteoporosis patients may help determine the pathogenesis of postmenopausal osteoporosis. In recent years, genetic testing technologies have been continuously developed and matured, with microarrays and high-throughput sequencing technologies employed to identify potential biomarkers related to the diagnosis, treatment and prognosis of osteoporosis [3–8]. Public databases are utilized to examine the diagnoses of multiple diseases and to identify prognostic biomarkers. In this study, the GSE68303 dataset was downloaded for bioinformatic analysis of differentially expressed genes between postmenopausal osteoporosis and control cases, and Interferon Regulatory Factor 4 (*IRF4*) emerged as a key gene in postmenopausal osteoporosis. However, few reports related to IRF4 and postmenopausal osteoporosis have been performed. Meanwhile, whether IRF4 could be used as a potential target to predict the occurrence of postmenopausal osteoporosis is undefined.

Interferon Regulatory Factors (IRFs) are DNA-binding proteins that belong to nuclear transcription factors, named after their regulatory effects on interferons [9]. The IRF family, including more than 10 members, is a group of widely expressed transcription factors originally reportedas downstream effectors of interferon signal transduction. IRF4 (also termed Pip, MUM1, LSIRF, NFEM5, or ICSAT), a major member of the IRF family, represents an essential immune regulator with close association with the differentiation of immune cells [10,11]. IRF4 is also considered a major regulator of abnormal and malignant tumor-specific genes in multiple myeloma, in which IRF4 is often overexpressed due to activated mutations or translocations [12,13]. Simulation experiments by *IRF4* gene manipulation indicated a sharp decline in the viabilityof multiple myeloma cells [13]. Mice lacking IRF4 in skeletal muscle showed a normal metabolic phenotype but re-

duced motility. Nakashima *et al*. [14] found that IRF4 is upregulated during RANKL (receptor activator of nuclear factor-κB ligand)-induced osteoclast differentiation, while simvastatin suppresses RANKL-triggered osteoclast genesis and downregulates nuclear factor of activated T-cells, cytoplasmic, calcineurin-dependent 1 (NFATc1), IRF4 and osteoclast markers. However, IRF4's impact on osteogenic differentiation in BM-MSCs remains undefined [15]. Postmenopausal osteoporosis is mainly associated with increased osteocyte activity, but whether IRF4 is related to postmenopausal osteoporosis is unknown. Simvastatin was reported to stimulate osteogenic differentiation in MSCs [16,17]. Furthermore, simvastatin significantly reduces osteoclast number and differentiation by stimulating IRF4 [14,18].

This study used bioinformatic analysis of the GSE68303 dataset, and cell culture and animal assays to confirm that IRF4 might be important in the pathogenesis of postmenopausal osteoporosis. The findings clarify IRF4's effects on PMOP, help understand IRF4's role in PMOP and provide new insights into the development of new treatment targets for PMOP.

2. Materials and Methods

2.1 Screening of DEGs in GEO

The GSE68303 datasets was downloaded from the Gene Expression Omnibus (GEO) database. GSE68303 datasets which contain 12 ovariectomize (OVX) experimental groups and 11 sham groups were downloaded. Then R software (R-4.3.1) was used to analyze the differentially expressed genes (DEGs) through the "Limma" package with $|\text{logFC}| \geq 0.5$ and $p < 0.05$ as criteria.

2.2 GO and KEGG Pathway Analysis.

Considering the retrieved DEGs, gene ontology (GO) and Kyoto Encyclopedia of Genes and Genomes (KEGG) pathway analyses were performed with the Enrichr database [19]. GO enrichment analysis encompassed terms related to biological process (BP), molecular function (MF), and cellular component (CC). KEGG pathway analysis is broadly employed for the identification of functional and metabolic pathways; here the threshold p value for statistical significance was 0.05.

2.3 PPI Network and Relative Expression of Hub Genes.

Search tool for the retrieval of interacting genes/proteins (STRING) was utilized to screen genes for protein-protein interaction (PPI) network generation, with an interaction of 0.4 selected. Visualization was carried out with Cytoscape 3.9.1 (http://www.cytoscape.org/). Hub genes were screened in CytoHubba by calculating the density of maximum neighborhood component (DMNC), Clustering Coefficient and edge percolated component (EPC). $p < 0.05$ indicated statistical significance.

2.4 Mouse Model

Female 8-week-old C57/BL6 mice order from Nanjing Medical University (Nanjing, China) were sham-operated or bilaterally ovariectomized (OVX) as described in a previous report [20]. After 8 weeks, successful ovariectomy was achieved as demonstrated by X-ray analysis of coccygeal vertebrae that showed significantly reduced bone mineral density (data not shown). Next, the OVX group was randomly subdivided into 2 groups of 6 each, administered water and simvastatin (Sigma, St. Louis, MO, USA) at 5 mg/kg/day, respectively, for 4 weeks. The simvastatin dose referred to a previous study [21]. After treatment, the vertebra were removed muscle and soft tissusses ,then collected and used to futhur analysised.

Housing was performed with 5 animals/cage, and a normal diet containing 1.0% calcium, 0.67% phosphorus, and 2.2 IU vitamin D/g was provided (#1010013; Jiangsu Province Collaborative Medicine Bioengineering, China). Assays involving animals were followed the ARRIVE guidelines (Animal Research: Reporting of *In Vivo* Experiments) [22] and approved by the Committee on the Ethics of Animal Experiments of Nanjing Medical University (Number: IACUC-1802007).

2.5 Bone Marrow Mesenchymal Stem Cells (BM-MSCs) Culture and Cytochemical Analysis

Tibiae and femurs from wild-type animals were obtained aseptically, and DMEM supplemented with 10% FBS, 50 µg/mL vitamin C (Sigma, USA), 10 mM β-glycerophosphate (Sigma, USA), and 10^{-8} M dexamethasone (Sigma, USA) was utilized to flush out bone marrow cells. After dispersion by repeated pipetting, single-cell suspensions were obtained by passing the cells through a 22G needle. This was followed by a 10–14 day culture in 6-well plates at 1 million cells per well in proliferation medium (2 mL), which was refreshed at 3-day intervals. Then, cells underwent a PBS wash, fixation with periodate-lysine-paraformaldehyde (PLP), and cytochemical staining for Alkaline phosphatase (ALP) [23] to detect ALP-positive CFU-f (CFU-fap). Briefly, following pre-incubation overnight with 1% magnesium chloride in 100 mM-Tris-maleate buffer (pH 9.2), dewaxed sections were incubated for 2 h at room temperature in 100 mM-Tris-maleate buffer containing naphthol AS-MX phosphate (0.2 mg/mL; Sigma, USA) dissolved in ethylene glycol monomethyl diethyl ether (Sigma, USA) as a substrate and fast red TR (0.4 mg/mL; Sigma, USA) as a stain for the reaction product.

2.6 Iconographic and Histopathological Assessments

Extracted femurs and tibias underwent micro–computed tomography [24], and histological, histochemical and immunohistochemical analyses [23]. Briefly, dewaxed and rehydrated paraffin-embedded sections were incubated with methanol: hydrogen peroxide (1:10) to

block endogenous peroxidase activity and then washed in Tris-buffered saline (pH 7.6). The slides were then incubated with the primary antibodies overnight at room temperature. After rinsing with Tris-buffered saline for 15 minutes, tissues were incubated with secondary antibody (biotinylated goat anti-rabbit IgG diluted 1:1000, Sigma-Aldrich, St. Louis, MO, USA). Sections were then washed and incubated with the Vectastain Elite ABC reagent (Vector Laboratories, Inc. Ontario, Canada) for 45 minutes. Staining was developed using 3,3-diaminobenzidine (2.5 mg/mL) followed by counterstaining with Mayer's Hematoxylin. Immunohistochemical staining employed anti-IRF4 (1:800) and anti-Runx2 (1:1000) primary antibodies (Abcam, Cambridge, UK). The staining pictures were taken by microscope (Olympus, Tokyo, Japan) equipted with image acquisition system (Nikon, Tokyo, Japan).

2.7 Immunoblot

Protein extraction from bone tissue samples followed a previous report [25]. Briefly, bone tissue samples were lysed in lysis buffer containing phenylmethylsulfonyl fluoride (PMSF) (Sigma, USA) supplemented with a protease inhibitor (Sigma, USA) or protease and phosphatase inhibitor cocktail (Roche, Indianapolis, IN, USA). The proteins were separated using gel electrophoresis and electrotransferred to polyvinylidene fluoride membranes. After blocking with 5% bovine serum albumin for 2 h and washing with Tris-buffered saline/Tween-20 (TBS-T) for 30 min, the membranes were incubated overnight at 4 °C with primary antibodies against anti-IRF4 (1:500, Abcam, USA) and anti-β-actin (1:1000, Bio world Technology, St Louis Park, MN, USA). Subsequently, the membranes were washed with TBS-T for 30 minutes at room temperature and incubated with horseradish peroxidase-conjugated secondary antibodies for 2 h. The membranes were then washed three times with TBS-T. Images of protein bands were obtained using the Chemi Doc XRS+ Imaging System (Bio-Rad, Hercules, CA, USA), and the densitometry values were analyzed by ImageJ (v1.53c, LOCI, University of Wisconsin, Madison, WI, USA). β-actin signals were employed for normalization.

2.8 Reverse Transcription Quantitative Real-Time Polymerase Chain Reaction (RT-qPCR)

Total RNA extraction from femur or BM-MSC samples used TRIzol reagent (Invitrogen, Waltham, MA, USA) as directed by the manufacturer. cDNA synthesis was carried out with the Prime Script RT Master Mix (Perfect Real Time; Takara, Kusatsu, Shiga, Japan). Agilent (Santa Clara, CA, USA) Touch Real-Time Detection System were used for RT-qPCR. The $2^{-\Delta\Delta CT}$ method was used as a relative quantification strategy for quantitative real-time polymerase chain reaction. Quantitative real-time RT-PCR was performed with the following primers:

IRF4: 5′-TCCGACAGTGGTTGATCGAC-3′, 5′-CTCACGATTGTAGTCCTGCTT-3′;

Runx2: 5′-ATGCTTCATTCGCCTCACAAA-3′, 5′-GCACTCACTGACTCGGTTGG-3′;

Alp: 5′-CTTGCTGGTGGAAGGAGGCAGG-3′, 5′-GGAGCACAGGAAGTTGGGAC-3′;

Ocn: 5′-GCTGCCCTAAAGCCAAACTCT-3′, 5′-GAGGACAGGGAGGATCAAGTTC-3′;

Col1a1: 5′-GCTCCTCTTAGGGGCCACT-3′, 5′-CCACGTCTCACCATTGGGG-3′.

2.9 Cell Transfection

BM-MSCs were cultured for 4 days, then the Lipofectamine 3000 kits (Invitrogen, USA) were used to transfect cells according to the manufacturer's instructions. Sh-IRF4, OV-IRF4, and negative control (NC) plasmids were purchased from Tran Sheep Bio Company (Shanghai, China). Tareget siIRF4-2 sequence: 5′-3′ CGGCACGCGGGGCATGAACCTGG, scrambled shRNA was used as a negative control. IRF4 cDNA primer Forward (5′-3′) GCTGATCGACCAGATCGACA Reverse (5′-3′) CGGTTGTAGTCCTGCTTGC. 24 h later, the culture medium was changed with 2 mL αMEM containing 10% FBS. Transfection efficiency could reach 63%–72% in cells detected by qRT-PCR after transfection of 25 nM Sh-IRF4, OV-IRF4 and NC plasmids using Lipofectamine 3000 according to the manufacturer's protocol.

2.10 Statistical Analysis

GraphPad Prism 6.07 (GraphPad Software, Inc., San Diego, CA, USA) was employed for data analysis. One-way ANOVA followed by Dunnett's multiple comparisons test was performed using GraphPad Prism Software, (Boston, MA USA, www.graphpad.com). All data were analyzed for normal distribution and presented as mean $\pm$ standard deviation (SD) from assays with n = 6/group. The unpaired *t*-test was performed for comparisons, and two-tailed $p < 0.05$ indicated statistical significance.

3. Results

GSE68303 datasets were used to explore the most valuable differential genes in postmenopausal osteoporosis. Then the difference in bone tissue expression between sham and ovariectomize (OVX) mice were analyzed. Western blot and immunohistochemical staining were used to detect the expression of IRF4 in thoracic vertebral extracts of OVX and Sham mice. BM-MSCs with IRF4 overexpressed (OV-IRF4) and knock down (Sh-IRF4) plasmids were constructed to the effect of IRF4 on osteogenic differentiation of postmenopausal osteoporosis.

3.1 DEGs in Postmenopausal Osteoporosis and Functional Enrichment Analysis of DEGs

To explore the most valuable differential genes in postmenopausal osteoporosis compared to control,

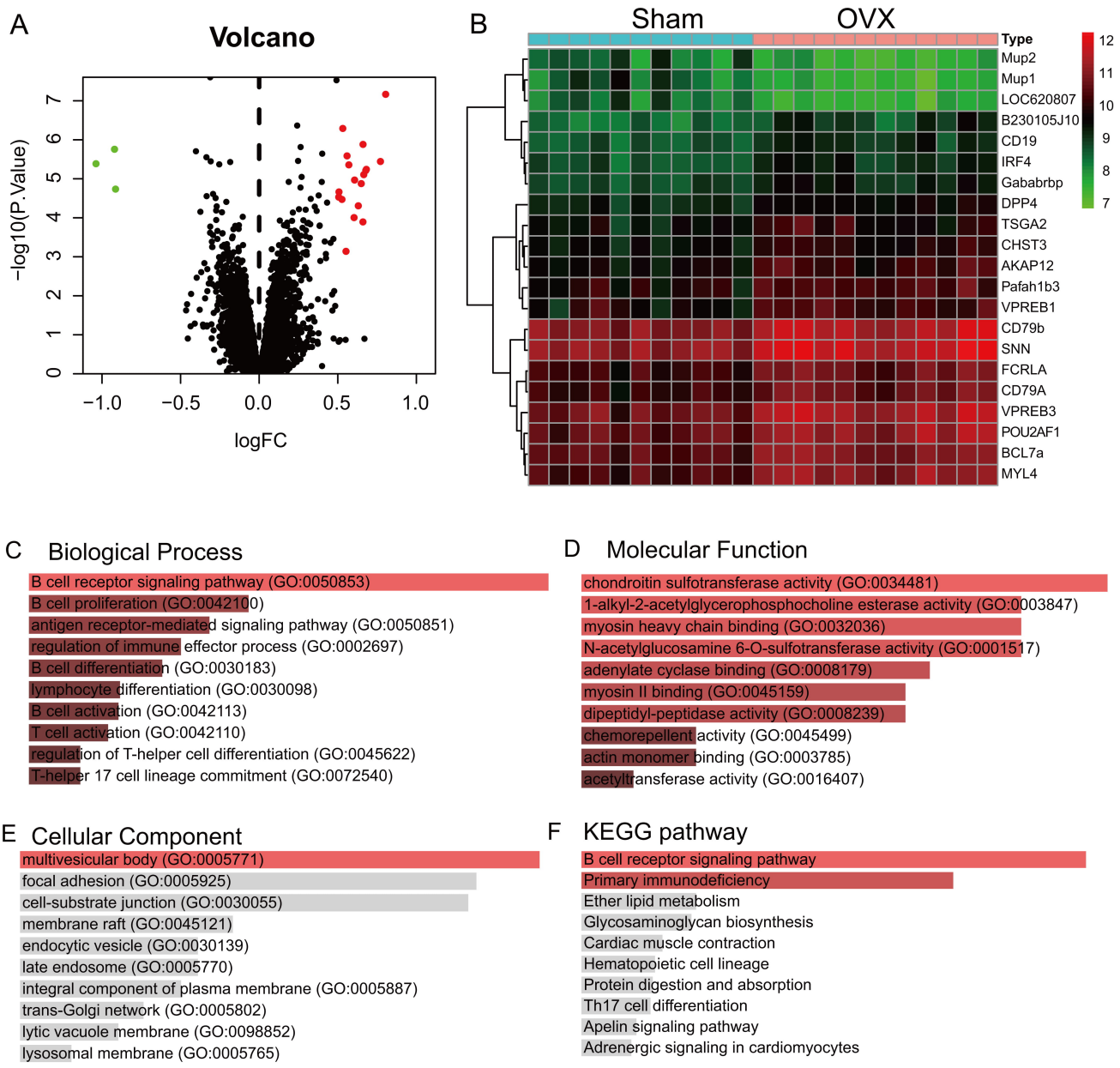

Fig. 1. The difference expressed genes (DEGs) in postmenopausal osteoporosis and functional enrichment analysis of the DEGs. (A) Volcano plot of DEGs between OVX and sham group. (B) The expression heatmap of DEGs. Red or green dots represent upregulated or downregulated genes, respectively. Genes without any significant difference are in black. The differences are set as $|\log FC| \geq 0.5$ and $p < 0.05$; GO and KEGG enrichment of the DEGs. (C) biological processes (D) molecular function (E) cellular component (F) KEGG pathway. OVX, ovariectomize; GO, gene ontology; KEGG, Kyoto Encyclopedia of Genes and Genomes.

GSE68303 datasets which contain 12 OVX experimental groups and 11 sham groups were downloaded. Then R software was used to analyze the differentially expressed genes (DEGs) through the "Limma" package and presented in the form of a Volcano Plot (Fig. 1A). The DEGs were screened with $|\log FC| \geq 0.5$ and $p < 0.05$. Finally, 3 DEGs that were down-regulated and 18 DEGs that were up-regulated were found and presented in the heatmap (Fig. 1B).

To better understand the function of the DEGs, the Enricher database [19] were used to analyze the GO enrichment and Kyoto gene and genome pathway encyclopedia (KEGG) enrichment. The main biological processes in which the DEGs were enriched are presented, including B cell receptor signaling pathway, B cell proliferation, and antigen receptor-mediated signaling pathway (Fig. 1C). Based on molecular function, DEGs were significantly enriched in chondroitin sulfotransferase activity,1-alkyl-2-acetylglycerophosphocholine ester activity, and myosin heavy chain binding (Fig. 1D). For cellular components, DEGs are specifically enriched in multivesicular bodies,

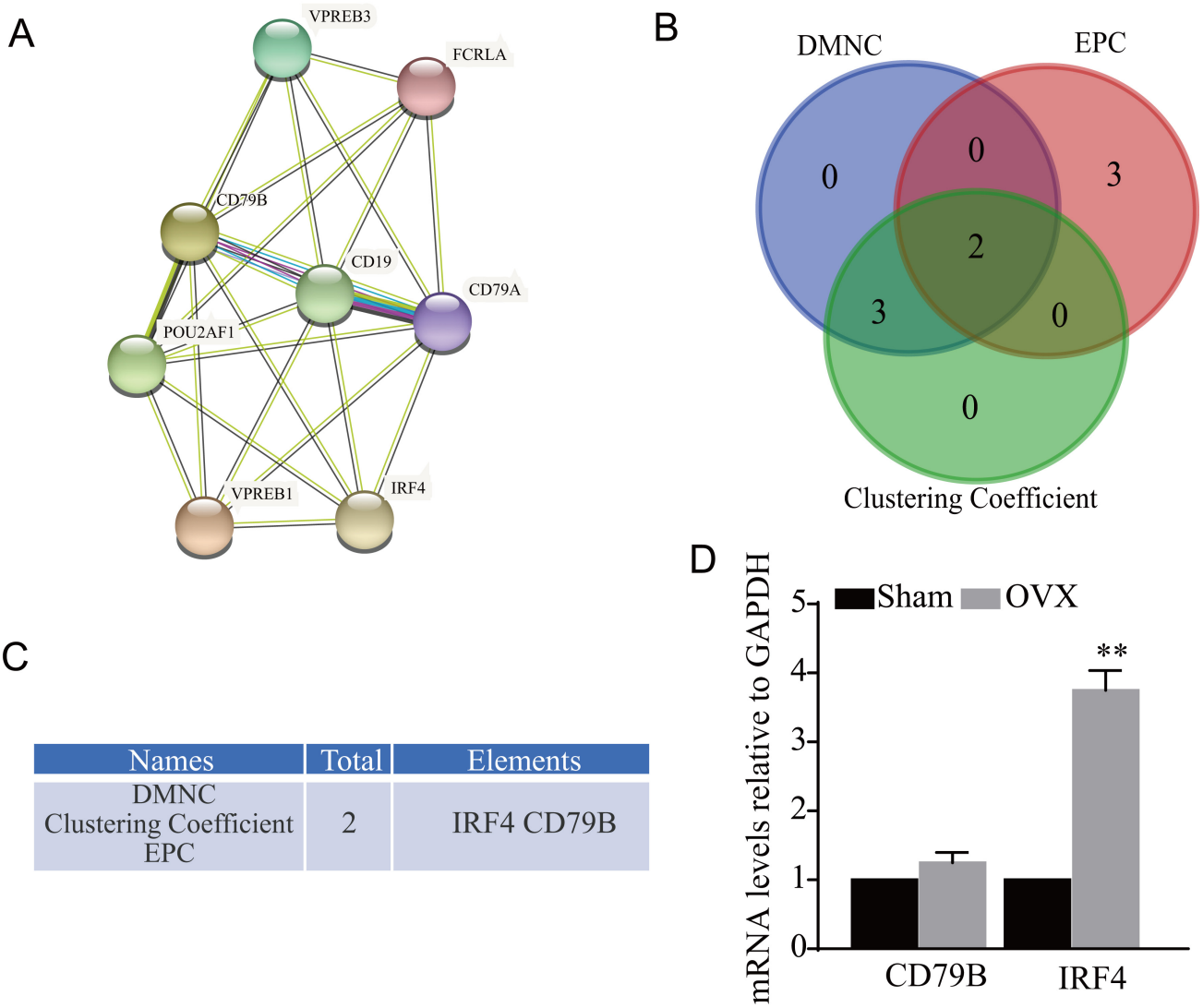

Fig. 2. Identification of the PPI networks and the hub genes. (A) The PPI network acquired from the String database. (B) Clustering Coefficient. (C) EPC of Cytoscape plugin cytoHubba. Two hub genes were selected by overlapping the top five genes based on three methods, including DMNC, Clustering Coefficient and EPC. (D) RT-qPCR of the mRNA exacted from OVX and Sham lumbar vertebrae. **, $p < 0.01$ compared with Sham group (n = 6). PPI, protein-protein interaction; EPC, edge percolated component; DMNC, density of maximum neighborhood component; RT-qPCR, reverse transcription quantitative real-time polymerase chain reaction; IRF4, interferon regulatory factor 4; mRNA, messenger RNA.

focal adhesions, and cellular substrate junctions (Fig. 1E). The KEGG pathways program was used to reveal the critical pathway, in which a total of 10 pathways were identified, such as B cell receptor signaling pathway, and pentose and glucuronate interconversion (Fig. 1F).

3.2 Identification of the PPI Networks and the Hub Genes

To determine potential associations among the retrieved DEGs, a PPI network was established in the STRING database based on protein interactions. By calculating the DMNC, Clustering Coefficient and EPC with the Cytoscope plugin cytoHubba, *IRF4* and *CD79B* were selected as the first two hub genes (Fig. 2A–C). In addition, RT-qPCR was used to quantitate their messenger RNA (mRNA) expression levels in lumbar vertebra samples from the OVX and Sham groups. The results revealed that IRF4 expression was significantly elevated in OVX animals in comparison with the Sham group (Fig. 2D). These results suggested that IRF4 might be a key regulator in the development of postmenopausal osteoporosis. Therefore, it was selected for further analysis.

3.3 IRF4 Is Essential in the Occurrence of Postmenopausal Osteoporosis

To further determine whether IRF4 plays a key role in postmenopausal osteoporosis, immunoblot was used to detect IRF4 protein expression in OVX and Sham mice firstly. As depicted in Fig. 3A,B, these results showed

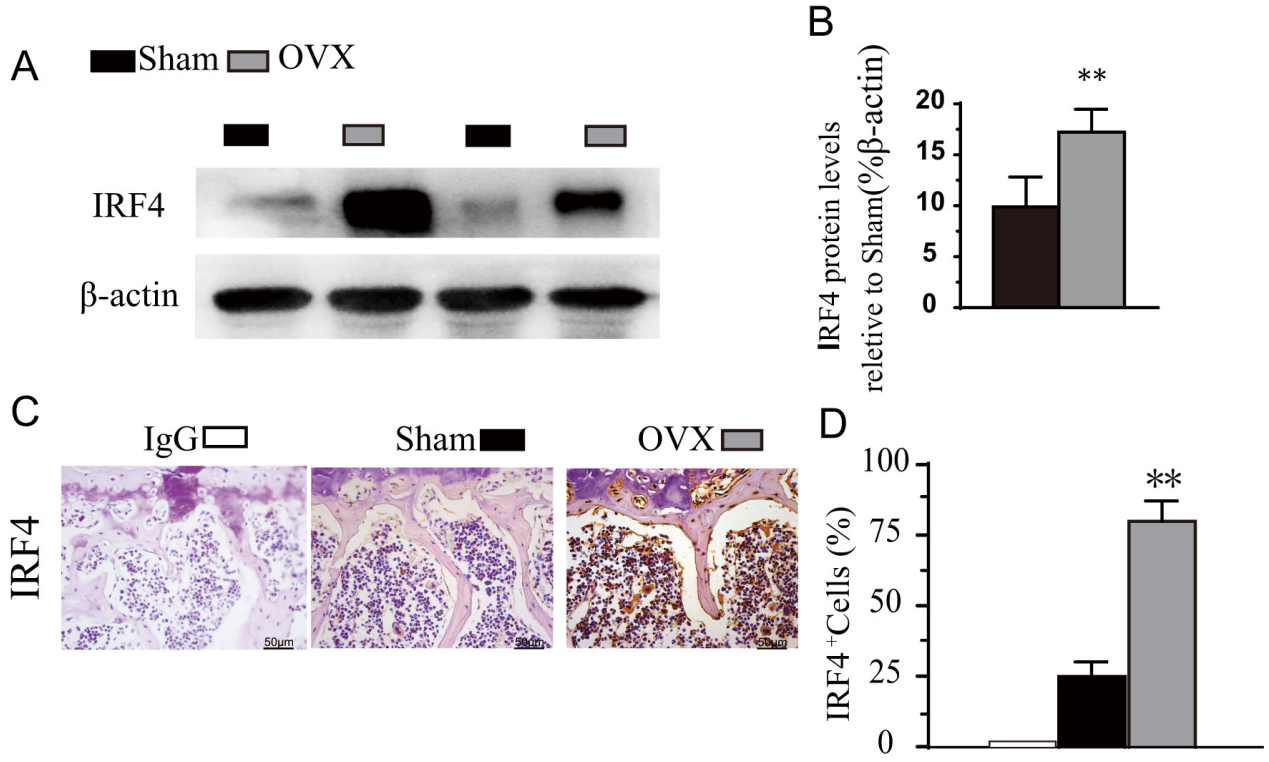

Fig. 3. IRF4 is essential in the occurrence of postmenopausal osteoporosis. (A) Western blots of IRF4 detected in thoracic vertebra extracts from OVX and Sham mice. (B) Protein level relative to β-actin assessed by densitometric analysis. (C) Representative micrographs from paraffin embedded sections of lumbar vertebrae stained immunohistochemically, 400×. (D) The percentage of IRF4 positive cells in the vertebrae tissues relative to total cells. Values are means ± standard deviation (SD) of six determinations per group. **, $p < 0.01$ compared with Sham group (n = 6).

that IRF4 protein expression was significantly elevated in OVX animals in comparison with the Sham group. Then immunohistochemical staining was used to detect IRF4 in lumbar vertebra samples from OVX and Sham mice. The results showed that IRF4-positive cells had significantly higher percentage in OVX animals versus the Sham group (Fig. 3C,D). These results suggest that IRF4 plays a crucial role in the pathogenetic mechanisms of postmenopausal osteoporosis.

3.4 IRF4 Overexpression Inhibits Osteogenic Differentiation of Postmenopausal BM-MSCs

To further study IRF4's impact on osteogenic differentiation in postmenopausal BM-MSCs, the latter cells were transfected with IRF4 overexpression (OV-IRF4) and knockdown (Sh-IRF4) plasmids, the efficiency of transfection for overexpression or silencing plasmids were showed in the **Supplementary Fig. 1**. As depicted in Fig. 4A,B, IRF4 overexpression significantly suppressed ALP activity, while IRF4 knockdown promoted ALP activity in BM-MSCs. These results indicate that IRF4 might regulate osteoporosis via inhibiting osteogenic differentiation in BM-MSCs.

To examine IRF4's role in PMOP-associated osteogenic differentiation, simvastatin (an inhibitor of IRF4) was used in OVX mice. After 4 weeks of treatment, Micro-CT examination was utilized to analyze bone density and bone volume fraction (BV/TV) after IRF4 inhibition. The results showed reduced bone density and BV/TV in the OVX group compared with Sham animals, while both indexes were significantly increased in simvastatin-treated OVX groups compared with the Sham and OVX groups (Fig. 4C–E). Meanwhile, immunohistochemical staining also showed that Runx2-positive cells (Fig. 4F,G) were significantly elevated in simvastatin-treated OVX groups. In OVX animals treated with simvastatin, osteogenic *Runx2*, *ALP*, type I collagen (*Col-I*) and osteocalcin (*OCN*) mRNA amounts were significantly elevated (Fig. 4H). These results suggest that IRF4 inhibition can prevent postmenopausal osteoporosis by inducing osteogenic differentiation in BM-MSCs.

4. Discussion

Postmenopausal osteoporosis represents the commonest primary osteoporosis, resulting in decreased estrogen secretion in postmenopausal women. To identify novel treatment targets, genes associated with postmenopausal osteoporosis were analyzed.

In this study, DEGs between sham and OVX mice in the GSE68303 dataset were screened, and 21 different

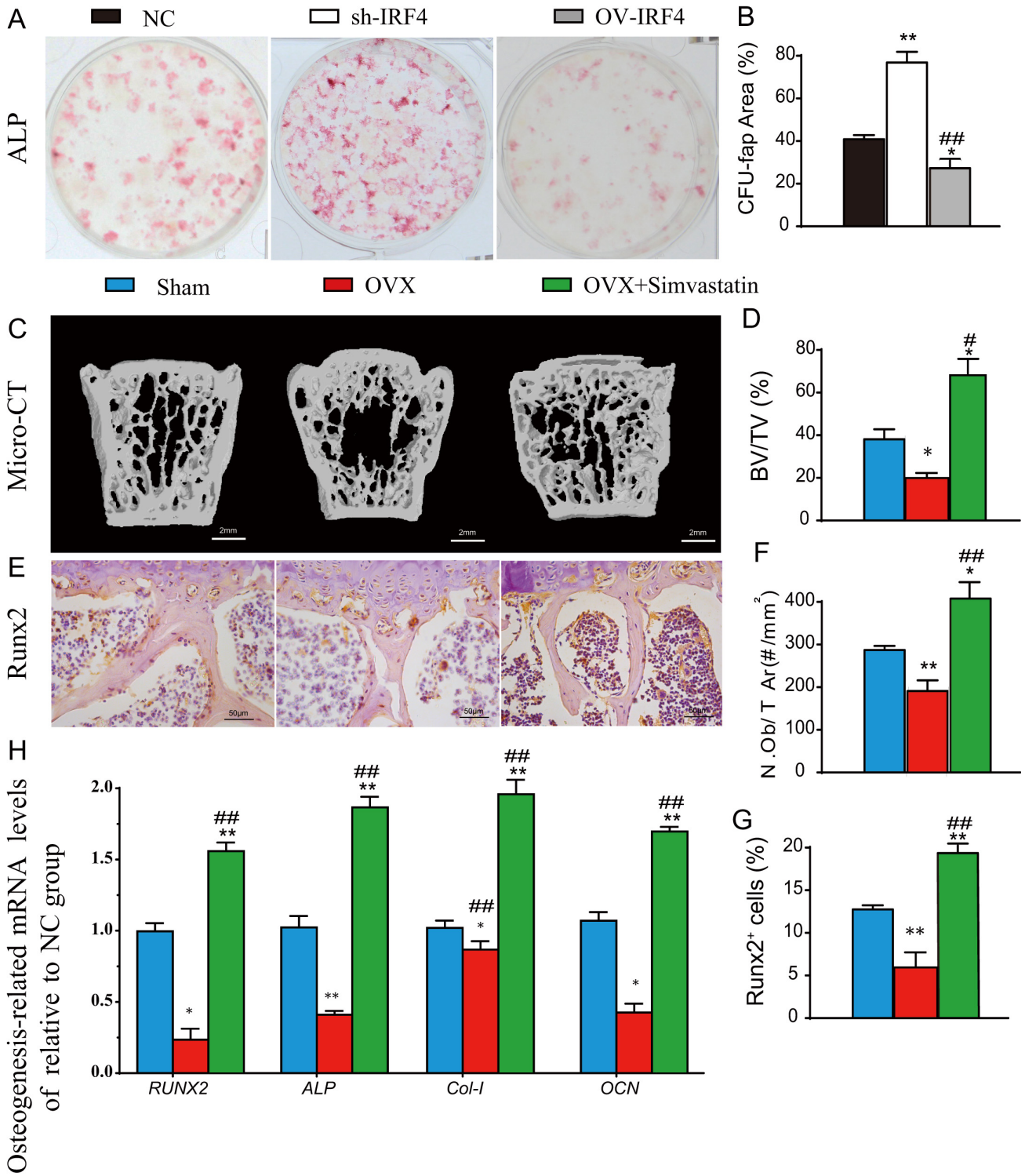

Fig. 4. IRF4 overexpression inhibits osteogenic differentiation of postmenopausal BM-MSCs. BM-MSCs of WT mice were transfected with OV-IRF4, Sh-IRF4 or NC and then were stained with alkaline-phosphatase (ALP) (A) and (B) CFU-f–positive areas. (C) Representative radiographs and three-dimensional reconstructions of Micro-CT. Quantitative bone formation analysis of the BV/TV (D) and N.Ob/T (E). Six animals were analyzed in each group. (F) Immunohistochemical staining of Runx2. (G) Runx2 positive cells (%). (H) Osteogenesis-related mRNA levels relative to NC group, *, $p < 0.05$, **, $p < 0.01$, compared with shame or NC group; #, $p < 0.05$, ##, $p < 0.01$, compared with sh-IRF4 or OVX group. BM-MSCs, bone marrow mesenchymal stem cells; WT, wild-type; CFU-f, colony-forming unit fibroblast; BV/TV, bone volume/total volume; N.Ob/T, osteoblast number/total area.

genes fulfilled the set criteria. GO and KEGG pathway analyses were performed. The data indicated that the important component of adaptive immunity may be a key regulator in postmenopausal osteoporosis. A PPI network was generated, and the first two hub genes, i.e., *CD79B* and *IRF4*, were identified by cell Hubba. Next, qPCR analysis indicated IRF4 was significantly upregulated in OVX mice compared with the Sham group, while CD79B expression had no statistically significant difference. These results implied that IRF4 is closely related to the onset of postmenopausal osteoporosis.

IRFs comprise nine members (IRF1-9), including a conserved N-terminal DNA-binding domain and a C-terminal regulatory domain [26]. They modulate immune cell development, differentiation, as well as responses to pathogens [26]. IRF4, produced by immune cells, activates or suppresses gene expression by delivering signals from various receptors. IRF4 is abnormally expressed in multiple lymphoid malignancies, and recent studies have revealed a crucial role for this protein in multiple myeloma development, while the relation between IRF4 and bone formation is quite unclear. IRF4 is associated with disease activity and pro-inflammatory cytokines, and constitutes a diagnostic marker of knee osteoarthritis in middle-aged and elderly people [27]. IRF4 suppresses osteogenic differentiation of BM-MSCs by transcriptionally activating miR-636/DOCK9 axis. It was disclosed that the inhibited osteogenic differentiation of BM-MSCs induced by IRF4 overexpression was rescued by miR-636 inhibition and IRF4/miR-636/DOCK9 axis was a promising target for the treatment of osteoporosis [15]. Previous reports [14] have shown that IRF4 is upregulated during RANKL-triggered osteoclast differentiation and may promote the transcription of osteoclast markers in the early stage of osteoclast formation. However, how IRF4 affects osteoblasts is rarely examined, so this study focused on its role in osteoblasts rather than osteoclasts.

Immunohistochemical staining and immunoblot were also utilized to confirm IRF4 expression in the vertebral bodies of Sham and OVX mice. As shown above, IRF4-positive cells had markedly elevated rate in OVX mice versus the Sham group. We believe that IRF4-positive cells were mostly BM-MSCs, and IRF4 mainly affected bone formation through the osteogenic differentiation of BM-MSCs. To assess whether knockdown of IRF4 can inhibit the osteogenic differentiation ability of BM-MSCs, WT BM-MSCs were transfected with NC, overexpression and knockdown IRF4 plasmids under osteogenic induction conditions, the results revealed that IRF4 overexpression inhibited the osteogenic differentiation ability of BM-MSCs, while IRF4 knockdown can promote the osteogenic differentiation. Previous paper also shows its function in osteogenic induction [15]. Simvastatin, which is known to inhibit IRF4 expression in many cells, such as T cells [28] and osteoclasts [14] and myeloid cells [29], was used in OVX mice to assess bone phenotype compared with Sham and OVX control mice, followed by Micro-CT analysis. All parameters evaluated revealed IRF4 inhibition in mice resulted in elevated bone density and mass in comparison with the Sham and OVX groups. The percentage of osteoblast cells expressing RUNX2 and the mRNA levels of osteogenic genes were markedly increased in OVX mice with IRF4 inhibition in comparison with the Sham and OVX groups. These results indicate that knockdown of IRF4 can promote BM-MSCs' osteogenic differentiation ability.

5. Conclusions

In conclusion, our study demonstrates that IRF4 is associated with postmenopausal osteoporosis. We found new effects of IRF4 affect bone stability by inhibiting the osteogenic differentiation ability of BM-MSCs, but due to some limitations, further study should be confirmed with clinical samples and more detailed mechanism needs to be explored. The results of this study also provide a new target for researching the occurrence and development of postmenopausal osteoporosis.

Abbreviations

IRF4, Interferon Regulatory Factor 4; BM-MSCs, bone marrow mesenchymal stem cells; PMOP, Postmenopausal osteoporosis; OVX, ovariectomy; OV-IRF4, IRF4 overexpressed; Sh-IRF4, IRF4 knock down; ALP, Alkaline phosphatase; RANKL, receptor activator of nuclear factor-κB ligand; NFATc1, nuclear factor of activated T-cells, cytoplasmic, calcineurin-dependent 1; MSCs, mesenchymal stem cells; GO, geneontology; KEGG, Kyoto Encyclopedia of Genes and Genomes; DMNC, Density of Maximum Neighborhood Component; EPC, Edge Percolated Component; CFU-f, colony-forming unit fibroblast; Runx2, runt-related transcription factor 2.

Availability of Data and Materials

The GSE68303 datasets was downloaded from the Gene Expression Omnibus (GEO) database. All datasets are already provided as part of the submitted article. The data and materials in the current study are available from the corresponding author on reasonable request.

Author Contributions

XiaoW designed the research study, Manuscript review, Funding support. XuanW and CY performed the research. XC provided help and advice on Literature search. ZS analyzed the data. XuanW, CY and ZS wrote the manuscript. All authors contributed to editorial changes in the manuscript. All authors read and approved the final manuscript. All authors have participated sufficiently in the work and agreed to be accountable for all aspects of the work.

Ethics Approval and Consent to Participate

Our study was approved by the Committee on the Ethics of Animal Experiments of Nanjing Medical University (Number: IACUC-1802007). At the end of the experiment, mice will be executed by CO_2, inhalation after halothane anesthesia, and then tissues and organs will be collected for other tests.

Acknowledgment

This work was supported by Research Center for Bone and Stem Cells; Key Laboratory for Aging & Disease.

Funding

This research was funded by the General Project of Nanjing Municipal Health Commission under Grant (YKK18244 to X.W.).

Conflict of Interest

The authors declare no conflict of interest.

Supplementary Material

Supplementary material associated with this article can be found, in the online version, at https://doi.org/10.31083/j.fbl2903115.

References

[1] Al-Anazi AF, Qureshi VF, Javaid K, Qureshi S. Preventive effects of phytoestrogens against postmenopausal osteoporosis as compared to the available therapeutic choices: An overview. Journal of Natural Science, Biology, and Medicine. 2011; 2: 154–163.

[2] Harvey N, Dennison E, Cooper C. Osteoporosis: impact on health and economics. Nature Reviews. Rheumatology. 2010; 6: 99–105.

[3] Low SS, Ji D, Chai WS, Liu J, Khoo KS, Salmanpour S, *et al*. Recent Progress in Nanomaterials Modified Electrochemical Biosensors for the Detection of MicroRNA. Micromachines. 2021; 12: 1409.

[4] Ye J, Xu M, Tian X, Cai S, Zeng S. Research advances in the detection of miRNA. Journal of Pharmaceutical Analysis. 2019; 9: 217–226.

[5] Kilic T, Erdem A, Ozsoz M, Carrara S. microRNA biosensors: Opportunities and challenges among conventional and commercially available techniques. Biosensors & Bioelectronics. 2018; 99: 525–546.

[6] Rauner M, Foessl I, Formosa MM, Kague E, Prijatelj V, Lopez NA, *et al*. Perspective of the GEMSTONE Consortium on Current and Future Approaches to Functional Validation for Skeletal Genetic Disease Using Cellular, Molecular and Animal-Modeling Techniques. Frontiers in Endocrinology. 2021; 12: 731217.

[7] Zhu X, Wang Z, Zhao Y, Jiang C. Investigation of candidate genes and mechanisms underlying postmenopausal osteoporosis using bioinformatics analysis. Molecular Medicine Reports. 2018; 17: 1561–1572.

[8] Calabrese G, Mesner LD, Foley PL, Rosen CJ, Farber CR. Network Analysis Implicates Alpha-Synuclein (Snca) in the Regulation of Ovariectomy-Induced Bone Loss. Scientific Reports. 2016; 6: 29475.

[9] Gualco G, Weiss LM, Bacchi CE. MUM1/IRF4: A Review. Applied Immunohistochemistry & Molecular Morphology: AIMM. 2010; 18: 301–310.

[10] Klein U, Casola S, Cattoretti G, Shen Q, Lia M, Mo T, *et al*. Transcription factor IRF4 controls plasma cell differentiation and class-switch recombination. Nature Immunology. 2006; 7: 773–782.

[11] Sciammas R, Shaffer AL, Schatz JH, Zhao H, Staudt LM, Singh H. Graded expression of interferon regulatory factor-4 coordinates isotype switching with plasma cell differentiation. Immunity. 2006; 25: 225–236.

[12] Wang L, Yao ZQ, Moorman JP, Xu Y, Ning S. Gene expression profiling identifies IRF4-associated molecular signatures in hematological malignancies. PLoS ONE. 2014; 9: e106788.

[13] Shaffer AL, Emre NCT, Lamy L, Ngo VN, Wright G, Xiao W, *et al*. IRF4 addiction in multiple myeloma. Nature. 2008; 454: 226–231.

[14] Nakashima Y, Haneji T. Stimulation of osteoclast formation by RANKL requires interferon regulatory factor-4 and is inhibited by simvastatin in a mouse model of bone loss. PLoS ONE. 2013; 8: e72033.

[15] Zhang X, Zhang Y, Yang L, Wu Y, Ma X, Tong G, *et al*. IRF4 suppresses osteogenic differentiation of BM-MSCs by transcriptionally activating miR-636/DOCK9 axis. Clinics (Sao Paulo, Brazil). 2022; 77: 100019.

[16] Zhang M, Bian YQ, Tao HM, Yang XF, Mu WD. Simvastatin induces osteogenic differentiation of MSCs via Wnt/β-catenin pathway to promote fracture healing. European Review for Medical and Pharmacological Sciences. 2018; 22: 2896–2905.

[17] Chuang SC, Liao HJ, Li CJ, Wang GJ, Chang JK, Ho ML. Simvastatin enhances human osteoblast proliferation involved in mitochondrial energy generation. European Journal of Pharmacology. 2013; 714: 74–82.

[18] Moon HJ, Kim SE, Yun YP, Hwang YS, Bang JB, Park JH, *et al*. Simvastatin inhibits osteoclast differentiation by scavenging reactive oxygen species. Experimental & Molecular Medicine. 2011; 43: 605–612.

[19] Kuleshov MV, Jones MR, Rouillard AD, Fernandez NF, Duan Q, Wang Z, *et al*. Enrichr: a comprehensive gene set enrichment analysis web server 2016 update. Nucleic Acids Research. 2016; 44: W90–W97.

[20] Shi C, Wu J, Yan Q, Wang R, Miao D. Bone marrow ablation demonstrates that estrogen plays an important role in osteogenesis and bone turnover via an antioxidative mechanism. Bone. 2015; 79: 94–104.

[21] Bonifacio A, Sanvee GM, Bouitbir J, Krähenbühl S. The AKT/mTOR signaling pathway plays a key role in statin-induced myotoxicity. Biochimica et Biophysica Acta. 2015; 1853: 1841–1849.

[22] Percie du Sert N, Hurst V, Ahluwalia A, Alam S, Avey MT, Baker M, *et al*. The ARRIVE guidelines 2.0: updated guidelines for reporting animal research. BMJ Open Science. 2020; 4: e100115.

[23] Wu J, Wang R, Kan X, Zhang J, Sun W, Goltzman D, *et al*. A Sonic Hedgehog-Gli-Bmi1 signaling pathway plays a critical role in p27 deficiency induced bone anabolism. International Journal of Biological Sciences. 2022; 18: 956–969.

[24] Sun W, Qiao W, Zhou B, Hu Z, Yan Q, Wu J, *et al*. Overexpression of Sirt1 in mesenchymal stem cells protects against bone loss in mice by FOXO3a deacetylation and oxidative stress inhibition. Metabolism: Clinical and Experimental. 2018; 88: 61–71.

[25] Miao D, Su H, He B, Gao J, Xia Q, Zhu M, *et al*. Severe growth retardation and early lethality in mice lacking the nuclear localization sequence and C-terminus of PTH-related protein. Proceedings of the National Academy of Sciences of the United States of America. 2008; 105: 20309–20314.

[26] Yanai H, Negishi H, Taniguchi T. The IRF family of transcription factors: Inception, impact and implications in oncogenesis. Oncoimmunology. 2012; 1: 1376–1386.
[27] Han W, Chen X, Wang X, Shen Z, Wang X, Zhang Z, *et al*. TLR-4, TLR-5 and IRF4 are diagnostic markers of knee osteoarthritis in the middle-aged and elderly patients and related to disease activity and inflammatory factors. Experimental and Therapeutic Medicine. 2020; 20: 1291–1298.
[28] Zhang X, Tao Y, Troiani L, Markovic-Plese S. Simvastatin Inhibits IFN Regulatory Factor 4 Expression and Th17 Cell Differentiation in CD4+ T Cells Derived from Patients with Multiple Sclerosis. The Journal of Immunology. 2011; 187: 3431–3437.
[29] Nam S, Kang K, Cha JS, Kim JW, Lee HG, Kim Y, *et al*. Interferon regulatory factor 4 (IRF4) controls myeloid-derived suppressor cell (MDSC) differentiation and function. Journal of Leukocyte Biology. 2016; 100: 1273–1284.